Early Postnatal Caloric Restriction Protects Adult Male Intrauterine Growth–Restricted Offspring From Obesity

Meena Garg,[1] Manikkavasagar Thamotharan,[1] Yun Dai,[1] Shanthie Thamotharan,[1] Bo-Chul Shin,[1] David Stout,[2] and Sherin U. Devaskar[1]

Postnatal ad libitum caloric intake superimposed on intrauterine growth restriction (IUGR) is associated with adult-onset obesity, insulin resistance, and type 2 diabetes mellitus (T2DM). We hypothesized that this paradigm of prenatal nutrient deprivation–induced programming can be reversed with the introduction of early postnatal calorie restriction. Ten-month-old male rats exposed to either prenatal nutrient restriction with ad libitum postnatal intake (IUGR), pre- and postnatal nutrient restriction (IPGR), or postnatal nutrient restriction limited to the suckling phase (50% from postnatal [PN]1 to PN21) (PNGR) were compared with age-matched controls (CON). Visceral adiposity, metabolic profile, and insulin sensitivity by hyperinsulinemic-euglycemic clamps were examined. The 10-month-old male IUGR group had a 1.5- to 2.0-fold increase in subcutaneous and visceral fat ($P < 0.0002$) while remaining euglycemic, insulin sensitive, inactive, and exhibiting metabolic inflexibility (V_{O_2}) versus CON. The IPGR group remained lean, euglycemic, insulin sensitive, and active while maintaining metabolic flexibility. The PNGR group was insulin sensitive, similar to IPGR, but less active while maintaining metabolic flexibility. We conclude that IUGR resulted in obesity without insulin resistance and energy metabolic perturbations prior to development of glucose intolerance and T2DM. Postnatal nutrient restriction superimposed on IUGR was protective, restoring metabolic normalcy to a lean and active phenotype. ***Diabetes*** **61:1391–1398, 2012**

A growing body of epidemiological observations and animal experiments has established the influence of intrauterine nutritional restriction and low birth weight on the later development of adult-onset metabolic disorders such as obesity, type 2 diabetes mellitus (T2DM), and dyslipidemia (1–5). Disruption of tissue-specific insulin-signaling pathways during the fetal and postnatal stages of development perturbs the whole-body glucose homeostasis, with concomitant insulin resistance in skeletal muscle and white adipose tissue (WAT) of the adult (1–3). We have previously demonstrated excessive weight gain and increased glucose-induced insulin release with emerging hepatic insulin resistance in female adult intrauterine growth–restricted (IUGR) rat offspring with ad libitum postnatal caloric intake (4). Undernutrition during gestation by itself led to increased hepatic glucose production (HGP) and impaired insulin signaling before the onset of obesity and diabetes in the adult male offspring (5). This presentation was distinct from the phenotype seen with postweaning high-fat diet consumption (6). Hyperglycemia and increased plasma insulin concentration with excessive total fat mass have previously been reported after ad libitum intake in 9-month-old IUGR male offspring that was further accentuated by increased dietary fat intake (6–8).

However, in large human observations, while small size at birth correlated with higher total fat mass, the resting metabolic rate per unit of fat-free mass also increased in young adults (9). While small size at birth may not necessarily reflect the nutritional state, it is not known whether this paradoxical increase in metabolic rate with increased adiposity is due to altered resting metabolic rate, metabolic fuel selection, or change in physical activity level. Based on these human observations, we examined distribution of body fat mass and metabolic profile in our previously described rat model of prenatal nutrient restriction with ad libitum postnatal calorie intake, restricted postnatal calorie intake, or postnatal calorie restriction alone (4).

We hypothesized that *1*) unrestricted postnatal caloric intake superimposed on nutrient restriction limited to late gestation and associated with IUGR would result in adult-onset obesity and glucose intolerance in the male offspring and *2*) early postnatal caloric restriction would protect the male IUGR offspring from developing adult-onset obesity and glucose intolerance. To test these hypotheses, we used the previously well-described rat model of caloric restriction during late gestation with cross-fostering allowing examination of four different groups, consisting of the control (CON) (gold standard), intrauterine growth restriction with postnatal ad libitum milk intake (IUGR), postnatal caloric limitation with growth restriction (PNGR), and combined IUGR with PNGR (IPGR).

RESEARCH DESIGN AND METHODS

Sprague-Dawley rats (Charles River Laboratories, Hollister, CA) were housed in individual cages, exposed to 12-h light/dark cycles at 21–23°C, and allowed ad libitum access to standard rat chow (composition carbohydrate 63.9%, fat 6.25%, and protein 18.6%). The National Institutes of Health guidelines were followed as approved by the animal research committee of the University of California, Los Angeles.

Animal model. We provided 50% of daily food intake (11 g/day) of a pregnant rat with ad libitum access to water from embryonic day (e)11 to e21, as we have previously described. This prenatal semi–nutrient restriction led to IUGR (3). At birth, the litter size was culled to six to ensure no interlitter nutritional variability. Postnatally, the cross-fostering of animals generated four experimental groups, as we have previously described (3). The newborn pups born to ad libitum–feeding control mothers were reared by either mothers continued on semi–nutrient restriction during lactation from postnatal (PN)1 to PN21 (PNGR) or by control mothers (CON) (Fig. 1*A*). During the suckling phase, the intrauterine semi–nutrient restriction progeny was fed and reared either by control mothers with ad libitum access to calories (IUGR), representing intrauterine nutrient restriction, or by semi–nutrient restriction mothers that continued to receive 50% of daily food intake (IPGR) during lactation, representing

From the [1]Division of Neonatology and Developmental Biology, Department of Pediatrics, Neonatal Research Center, David Geffen School of Medicine at University of California, Los Angeles, Los Angeles, California; and the [2]Crump Institute for Molecular Imaging, David Geffen School of Medicine at University of California, Los Angeles, Los Angeles, California.
Corresponding author: Sherin U. Devaskar, sdevaskar@mednet.ucla.edu.
Received 28 September 2011 and accepted 18 February 2012.
DOI: 10.2337/db11-1347

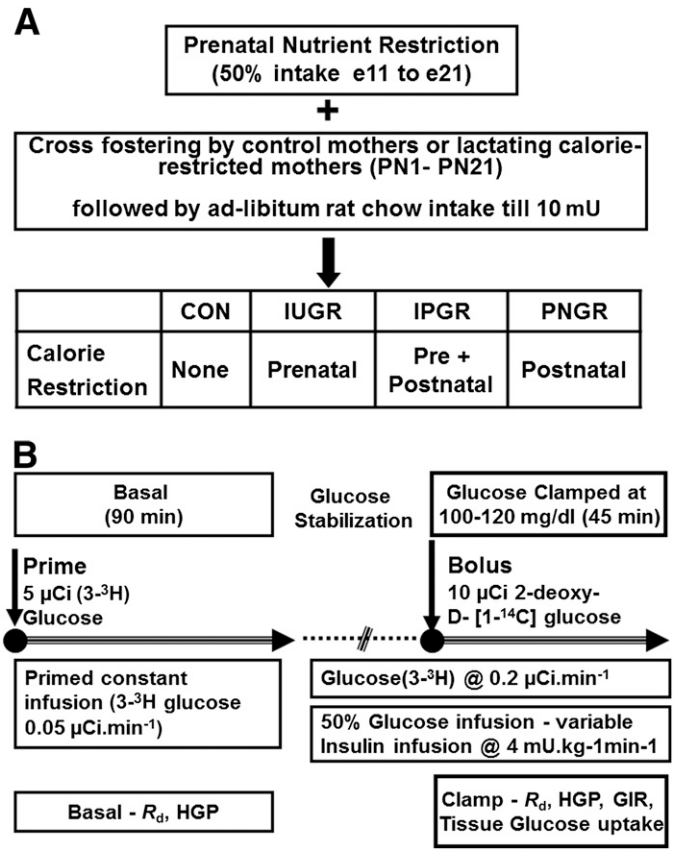

FIG. 1. *A*: Experimental groups are depicted schematically. *B*: Experimental design, hyperinsulinemic-euglycemic clamp study. mU, milliunits.

intrauterine with superimposed postnatal nutrient restriction. All four groups had ad libitum access to water and rat chow after weaning from dams until the time of study at 10 months of age. In this study, only the male offspring were examined.

Abdominal computed tomography. The animals were anesthetized by an initial intraperitoneal injection containing mixture of ketamine and xylazine (50 + 4.8 mg/kg) followed by inhaled 2% isoflurane per 2.5 L oxygen delivered by a nose cone during the entire procedure. The animals were placed supine in the micro–computed tomography scanner (MicroCAT II system; Siemens Preclinical Solutions, Knoxville, TN). Images were created using a Feldkamp reconstruction algorithm to a 400-micron voxel size and 800-micron resolution. The subcutaneous and visceral fat areas were measured on one cross-sectional scan obtained at the constant level of the fifth lumbar vertebra. The intraperitoneal and subcutaneous fat tissue was assessed by the region-of-interest (ROI) analysis. Total fat area was calculated by counting the number of pixels in each ROI, i.e., total fat and the visceral fat areas. Subcutaneous fat area was assessed by subtracting visceral fat from the total fat areas (10).

Food and water intake. Body weight and food and water intake were recorded in 15 postweaned animals from each group over a period of 24 h at intervals of 1 month, taking into account food spillage and evaporation.

Energy expenditure and respiratory exchange ratios. An indirect open-circuit calorimeter (Oxymax; Columbus Instruments, Columbus, OH) was used for these measurements in 10-month-old males in all four groups (11). The calorimeter was calibrated, and rats were weighed and placed individually in sealed chambers. Rats were conscious and unrestrained during the measuring period. All measurements were made simultaneously in the fed state with ad libitum access to food and water and after an overnight fast with free access to water only. After an optimal acclimation period of 24 h, the calorimeter airflow rate was adjusted according to the animal weight. The expired air was analyzed for a 30-s period every 6 min using an electrochemical O_2 analyzer and a CO_2 sensor (Oxymax). V_{O_2} and V_{CO_2} were measured by the indirect calorimeter and expressed as milliliters of $O_2 \times hour^{-1} \times$ body weight in kilograms (11,12). The respiratory exchange ratio (RER) was calculated as V_{CO_2}/V_{O_2} (volume of CO_2 produced per volume of O_2/CO_2 consumed [milliliters per kilogram per minute]). Energy expenditure (kilocalories per kilogram per hour; heat production) was calculated using a rearrangement of the Weir equation as supplied by Columbus Instruments: $(3.815 + 1.232 \times RER) \times V_{O_2}$ (11,13). A mean of 12–14 determined values per rat was averaged for the final value. ($n = 6$ in each group.) Analysis of the substrate used for oxidation was derived based on the RER values using Table 1 of a previously published article (14). As a control, resting V_{O_2} measured during none to less than baseline activity (0–10 counts/10 min) (12) served as a measure of basal or resting metabolic rate.

Activity scoring. Oxymax (Opto-M3 Activity Monitor) with 16 infrared (IR) beams intersecting the chamber in the *x*-, *y*-, and *z*-axes was used to obtain activity counts associated with ambulation. IR photocells were placed at a height above the animal (*z*-axis) to detect activities of rearing or jumping. The activity data were obtained concurrently during the period of calorimetric measurements and were averaged every 10 min. Calorimeter was configured for *x*, *xy*, *xz*, or *xyz* coverage. Each interruption of IR beams in *x*- and *y*-axes accrued a count of activity, and *z*-axis counted rearing (12).

Intravenous glucose tolerance tests. Adult awake 10-month-old male animals received 0.5 g/kg glucose via the tail vein, and blood was obtained at 0, 5, 15, 30, 60, and 120 min subsequently to measure plasma glucose and insulin concentrations. The insulin concentrations measured at 5 min following the intravenous glucose challenge reflected the first phase and were used to determine the glucose-stimulated insulin release (GSIR).

Hyperinsulinemic-euglycemic clamp studies

Surgical catheter placement. Ten-month-old adult male rats were anesthetized using inhalational isoflurane. One week prior to the clamp studies, catheters were inserted into two jugular veins and right carotid artery, tunneled subcutaneously, exteriorized, and maintained patent with heparinized saline. Pain was controlled with ketoprofen (10 mg/kg), and antibiotics (50 mg/kg ampicillin) were given daily for the first 48 h after surgery. Only animals that recovered adequately and were active and eating normally after the surgery were used in the clamp experiments.

Hyperinsulinemic-euglycemic clamp experiments. All animals were subjected to an overnight fast for ~16 h prior to the clamp to standardize liver glycogen and hepatic glucose output. Under basal conditions, the animals received a primed (5 μCi bolus) constant intravenous infusion of [3-^{3}H]glucose (0.05 μCi/min) over 90 min to achieve steady state (Fig. 1*B*). For creation of the hyperinsulinemic-euglycemic clamp condition, rats then received an intravenous infusion of insulin (Novolin R, regular human insulin, recombinant DNA origin; Novo Nordisk) at 4 mU/kg/min with continuation of the (3-^{3}H)glucose (0.2 μCi/min) infusion to maintain the achieved steady state (Fig. 1*B*). A variable infusion of 50% glucose solution was started at the beginning of the hyperinsulinemic clamp and adjusted to maintain the plasma glucose concentration at 100–120 mg/dL (euglycemia). Insulin-stimulated tissue glucose uptake was simultaneously estimated by the concomitant administration of an intravenous bolus of the nonmetabolizable 2-deoxy-D-[1-^{14}C]glucose (10 μCi; Perkin Elmer). Blood sampling was performed every 10 min over a 45-min

TABLE 1
Body weight, plasma insulin and leptin concentration, and food and water intake corrected for body weight in 10-month-old male animals after an overnight fasting state

Body weight (g)		Glucose (mg/dL)	Insulin (ng/mL)	Leptin (ng/mL)	Food intake/100 g body wt (g)[a]	Body weight/FI (g/g)[b]	Water intake/body weight (g)
CON (15)	784.3 ± 21.0	134.6 ± 10.3	1.8 ± 0.2	20.0 ± 3.7	3.0 ± 0.2	34.8 ± 3.1	0.037 ± 0.005
IUGR (16)	841.2 ± 22.2*†‡	157.2 ± 22.1	1.8 ± 0.2	32.0 ± 3.9*†‡	2.8 ± 0.3‡‡	37.1 ± 2.6	0.037 ± 0.006
IPGR (15)	663.5 ± 14.4**	146.0 ± 6.8	1.7 ± 0.2	15.9 ± 2.1###	3.4 ± 0.4	29.8 ± 1.8	0.0423 ± 0.006
PNGR (15)	664.1 ± 11.9**	123.1 ± 9.9	0.9 ± 0.1*#††	10.5 ± 0.7###	3.9 ± 0.3*	27.2 ± 2.5##	0.048 ± 0.009

Data are means ± SD. [a]Food intake per 100 g body wt as assessed over a 24-h period at 10 months of age alone is shown. [b]Body weight per gram of food intake (FI) reflects the caloric efficiency. *$P < 0.03$ vs. CON. †$P < 0.0001$ vs. IPGR. ‡$P < 0.001$ vs. PNGR. ‡‡$P < 0.008$ vs. PNGR. **$P < 0.0001$ vs. CON. ###$P < 0.001$ vs. IUGR. #$P < 0.05$ vs. IUGR. ††$P < 0.002$ vs. IPGR. ##$P < 0.02$ vs. IUGR.

period after achieving clamp conditions. At the end of the clamp study, rats were killed with pentobarbital sodium (150 mg/kg i.v.) and the collected tissues were snap-frozen in liquid nitrogen for subsequent analysis.

Total-body glucose kinetics. Plasma samples were analyzed for glucose concentration by a HemoCue glucose 201 analyzer (HemoCue, Cypress, CA). [3-^{3}H]glucose specific radioactivity was assessed in the supernatant of barium hydroxide–zinc sulfate–precipitated plasma samples after overnight elimination of tritiated water (Somogyi method) by evaporating to dryness. In steady state, the R_a of glucose, which equals R_d, was calculated by dividing the infusion rate of labeled glucose by the specific activity at the same time point. Endogenous HGP was calculated by subtracting the unlabeled glucose infusion rate (GIR) from R_d.

Tissue glucose uptake. Tissue samples, which included the liver, white fat, soleus muscle, extensor digitorum longus muscle, and gastrocnemius, were treated with 1 mol/L NaOH at 60°C for 45 min. These tissue extracts were neutralized with 1 mol/L HCl prior to deproteination by 6% $HClO_4$ and $Ba(OH)_2$/$ZnSO_4$ precipitation separately. The supernatants were collected by centrifugation at 5,000*g* for 5 min, and the radioactivity associated with total and free 2-deoxyglucose was measured. Tissue 2-deoxyglucose-6-PO_4 concentration was calculated as the difference between total ($HClO_4$ supernatant) and free 2-deoxyglucose [$Ba(OH)_2$/$ZnSO_4$ supernatant] radioactivity.

Plasma assays. Plasma was separated, and aliquots were prepared for measurement of glucose by the glucose oxidase method (Sigma Diagnostics, St. Louis, MO) (sensitivity = 0.1 mmol/L). Insulin and leptin were quantified by enzyme-linked immunosorbent assays using rat standards and anti-rat insulin or leptin antibodies (Linco Research, St. Charles, MO) (sensitivity: insulin = 0.2 ng/mL, leptin = 0.04 ng/mL using 10-μL sample).

Data analysis. All data are expressed as means ± SE. The ANOVA models were used for normal distribution of data to compare the various treatment groups at different ages and *F* values determined. Intergroup differences were validated by the post hoc Fisher paired least significant differences test. Comparison of the fasted with the fed states between the four experimental groups was conducted by two-way ANOVA for measurements of V_{O_2}, V_{CO_2}, heat production, resting energy ratio, and activity. Similarly, comparison between basal and hyperinsulinemic-euglycemic clamp conditions (R_d, HGP, and GIR) of the four experimental groups was conducted by two-way ANOVA, and pairwise comparisons were performed using the post hoc Tukey test. Significance was assigned when *P* values were <0.05.

RESULTS

Anthropometric measurements, food and water intake, plasma glucose, and hormone concentrations. From 4 to 10 months of age, the IUGR male weighed significantly more than CON, while IPGR and PNGR were lighter than CON and IUGR (Fig. 2*A* and Table 1). Body weight at weaning (21 days) in IUGR, IPGR, and PNGR was uniformly lower than that of the age-matched CON ($P < 0.0001$) (Fig. 2*A*). This weight gain by 10-month-old IUGR was associated with a lower food intake (per 100 g body wt) versus that of 10-month-old PNGR ($P < 0.008$) (Table 1) and achieved statistical significance the earliest at 6 months of age ($P < 0.001$) (Fig. 2*A*). In contrast, the lighter PNGR demonstrated a higher food intake per unit body weight compared with CON ($P < 0.03$) and IUGR ($P < 0.008$) at 10 months (Table 1). There were no differences in water intake between the four groups (Table 1). The caloric efficiency determined as body weight/food intake (defined as the body weight achieved per unit caloric intake) in IUGR and IPGR groups was similar to CON but was lower in PNGR versus that in IUGR (Table 1). Further, the PNGR group demonstrated the lowest caloric efficiency (body weight/food intake) and was statistically significant compared with the IUGR group ($P < 0.02$) (Table 1). While intergroup baseline glucose concentrations were not different, plasma insulin concentration in the PNGR group was significantly lower than in the CON ($P < 0.3$), IUGR ($P < 0.5$), and IPGR ($P < 0.002$) groups. The plasma leptin concentrations were higher in IUGR than in CON ($P < 0.03$), IPGR ($P < 0.0001$), and PNGR ($P < 0.001$) (Table 1).

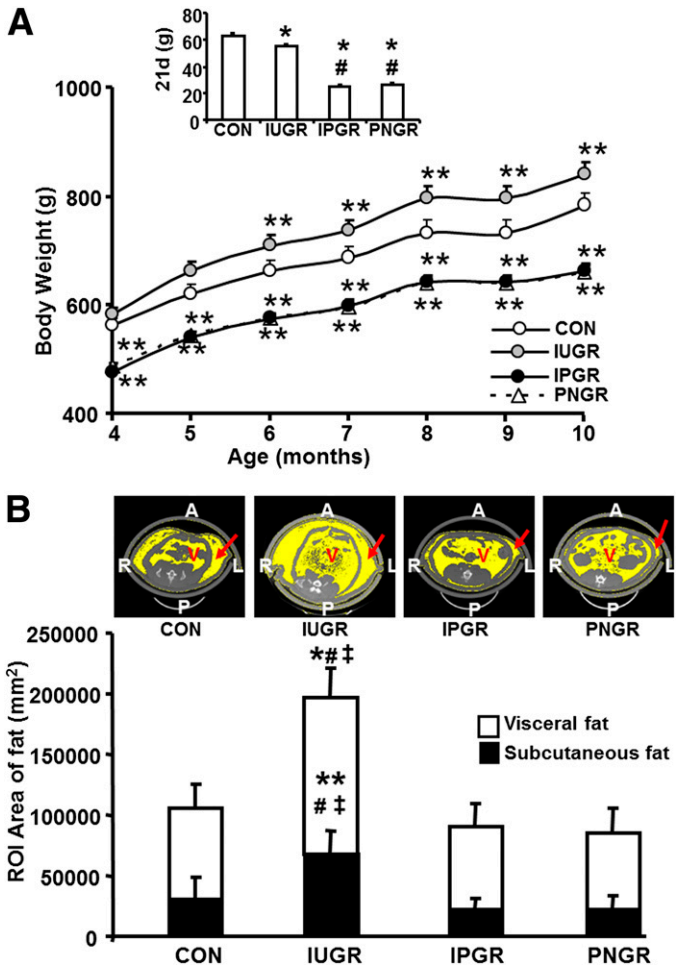

FIG. 2. ***A*: The weight gain in CON, IUGR, IPGR, and PNGR is shown from 4 to 10 months of age. The inset shows body weight at 21 days (d) for the four groups. *$P < 0.0001$ IUGR, IPGR, and PNGR vs. CON (inset); #$P < 0.0001$ IPGR and PNGR vs. IUGR (inset); **$P < 0.001$ IUGR, IPGR, and PNGR vs. CON. *B*: Quantification by ROI analysis of subcutaneous and visceral fat is shown in CON, IUGR, IPGR, and PNGR; $n = 6$ for each group. The inset shows the representative transverse section images of abdominal computed tomography scans for each group at 10 months of age. Arrow points to the subcutaneous fat. A, anterior; L, left; P, posterior; R, right; V, visceral. **$P < 0.0004$, *$P < 0.0002$ IUGR vs. CON; #$P < 0.0001$ IUGR vs. IPGR; ‡$P < 0.0001$ IUGR vs. PNGR. (A high-quality color representation of this figure is available in the online issue.)**

Assessment of visceral and subcutaneous fat. Computed tomography scan ROI analysis quantified (Fig. 2*B*) a significant increase in subcutaneous ($P < 0.0004$) and visceral ($P < 0.0002$) fat in the IUGR group, reflecting the increased plasma leptin concentration (Table 1) compared with CON, IPGR ($P < 0.0001$ for subcutaneous and visceral), and PNGR groups ($P < 0.0001$ for subcutaneous and visceral). Representative computed tomography scans at the level of L5 are depicted in the inset of Fig. 2*B*. In contrast, while there is an apparent qualitative decrease in subcutaneous fat and increase in visceral fat of the PNGR and IPGR versus CON (Fig. 2*B*) groups, ROI quantification did not reveal any significant difference (Fig. 2*B*).

V_{O_2}, heat production, V_{CO_2}, RER, and activity. After an overnight fast, V_{O_2} (milliliter per kilogram per hour) in all three groups was similar to that in CON (Fig. 3*A*). However, after feeding, the IUGR group failed to increase V_{O_2} (Fig. 3*A*) and heat production (kilocalories per kilogram per hour) (Fig. 3*B*), which we referred to as "metabolic

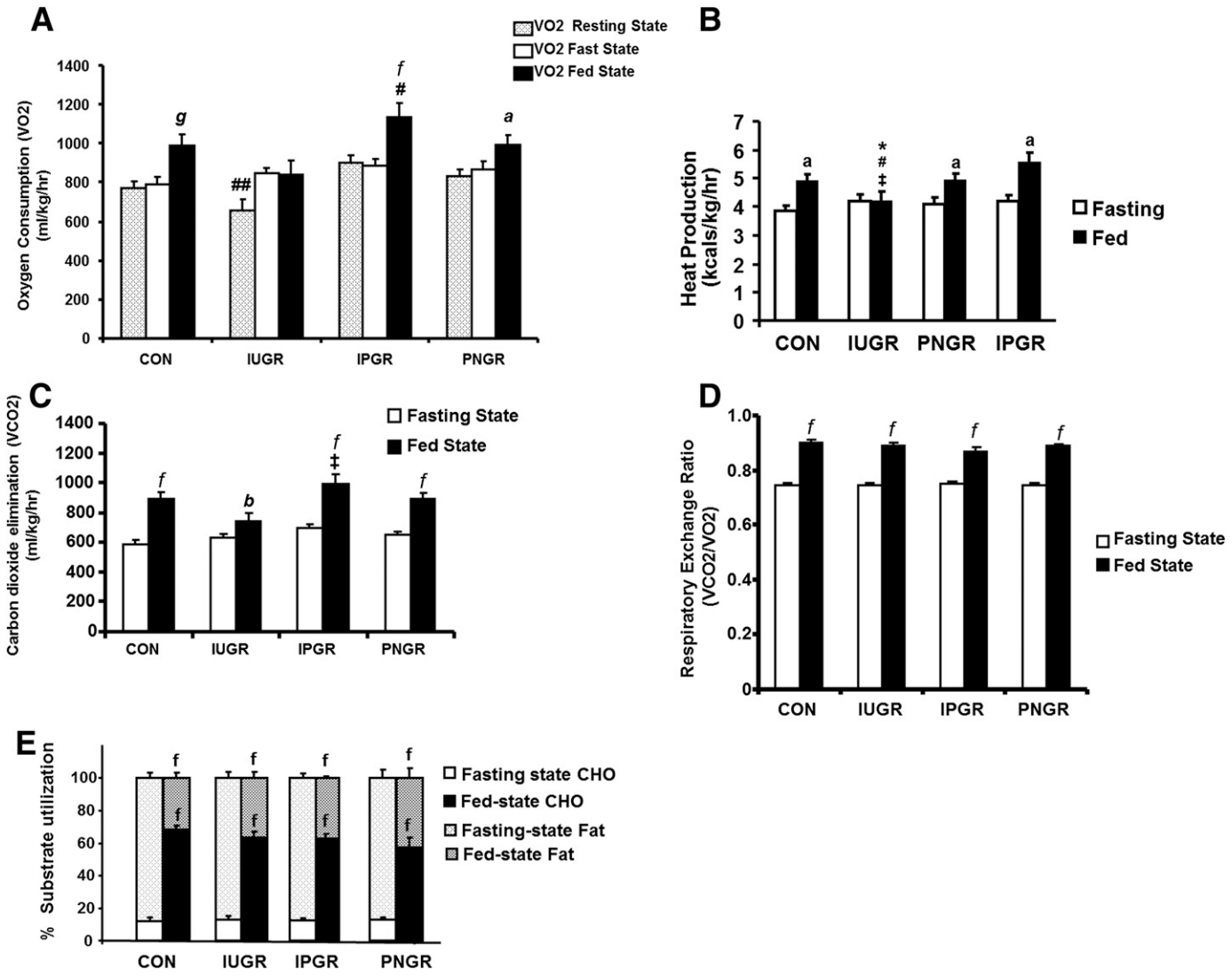

FIG. 3. *A*: VO_2. *B*: Heat production. *C*: VCO_2. *D*: RER. *E*: Percent use of substrates carbohydrate (CHO) and fat is shown in IUGR, IPGR, PNGR, and CON groups during fasting and fed states ($n = 6$ in each group). Fasting vs. fed states in the respective groups: $^aP < 0.01$, $^bP < 0.02$, $^fP < 0.001$, $^gP < 0.003$. #$P < 0.001$ VO_2 fed-state IPGR vs. fasting and fed states in IUGR group. ##$P < 0.05$ resting-state VO_2 IUGR vs. resting-state VO_2 IPGR. *$P < 0.03$ heat production during fed state in the IUGR vs. the fed state in CON. #$P < 0.0003$ heat production during fed state in the IUGR vs. fed state in CON. ‡$P < 0.02$ heat production during fed state in PNGR vs. fed state in IUGR. ‡$P < 0.001$ VCO_2 fed state in IPGR vs. fed state in IUGR.

inflexibility," while the IPGR ($P < 0.001$) and PNGR ($P < 0.01$) groups showed a significant increase in VO_2 and heat production (IPGR $P < 0.04$ and PNGR $P < 0.05$) similar to CON ($P < 0.003$) (Fig. 3*A* and *B*). In the IPGR, VO_2 during the fed state was significantly higher than VO_2 in both fasting and fed states of the IUGR group ($P < 0.001$) (Fig. 3*A*). Resting VO_2 was measured as a reflection of basal metabolic rate assessed during the resting state consisting of none to less than baseline activity (0–10 counts/10 min) and observed to be lower in IUGR versus CON, IPGR, and PNGR, only achieving statistical significance compared with the IPGR group ($P < 0.05$) (Fig. 3*A*). The IUGR group demonstrated lower heat production in the fed state compared with CON, IPGR, and PNGR (Fig. 3*B*). In contrast to VO_2, VCO_2 showed an appropriate increase in the fed state versus the fasted state in all experimental groups (IUGR $P < 0.02$; IPGR and PNGR $P < 0.001$), similar to that of CON ($P < 0.001$) (Fig. 3*C*), although the IUGR demonstrated the least increase. The resting energy ratio (VCO_2/VO_2) was higher after feeding in all groups, similar to CON ($P < 0.001$) (Fig. 3*D*). Additionally, an expected significant increase in percent of energy generated from carbohydrate ($P < 0.001$) after feeding but from fat during the fasting state ($P < 0.001$) was noted in all four groups (Fig. 3*E*).

The total, rearing, and ambulatory activity counts averaged over 10-min epochs showed increase in IPGR ($P < 0.02$, 0.003, and 0.02, respectively) during the fed versus the fasted states, similar to that seen in CON (Fig. 4*A–C*). The total activity of the IUGR that demonstrated metabolic inflexibility and that of the PNGR that exhibited caloric inefficiency were no different between the fed and fasted states (Fig. 4*A–C*).

Glucose tolerance test and GSIR. Plasma glucose and glucose area under the curve (AUC) in IUGR, IPGR, and PNGR were not different from CON (Fig. 5*A* and *B*). GSIR at 5 min after a glucose challenge in IPGR was significantly higher than in CON ($P < 0.03$), IUGR ($P < 0.005$), and PNGR ($P < 0.003$) (Fig. 5*C*). This resulted in total insulin

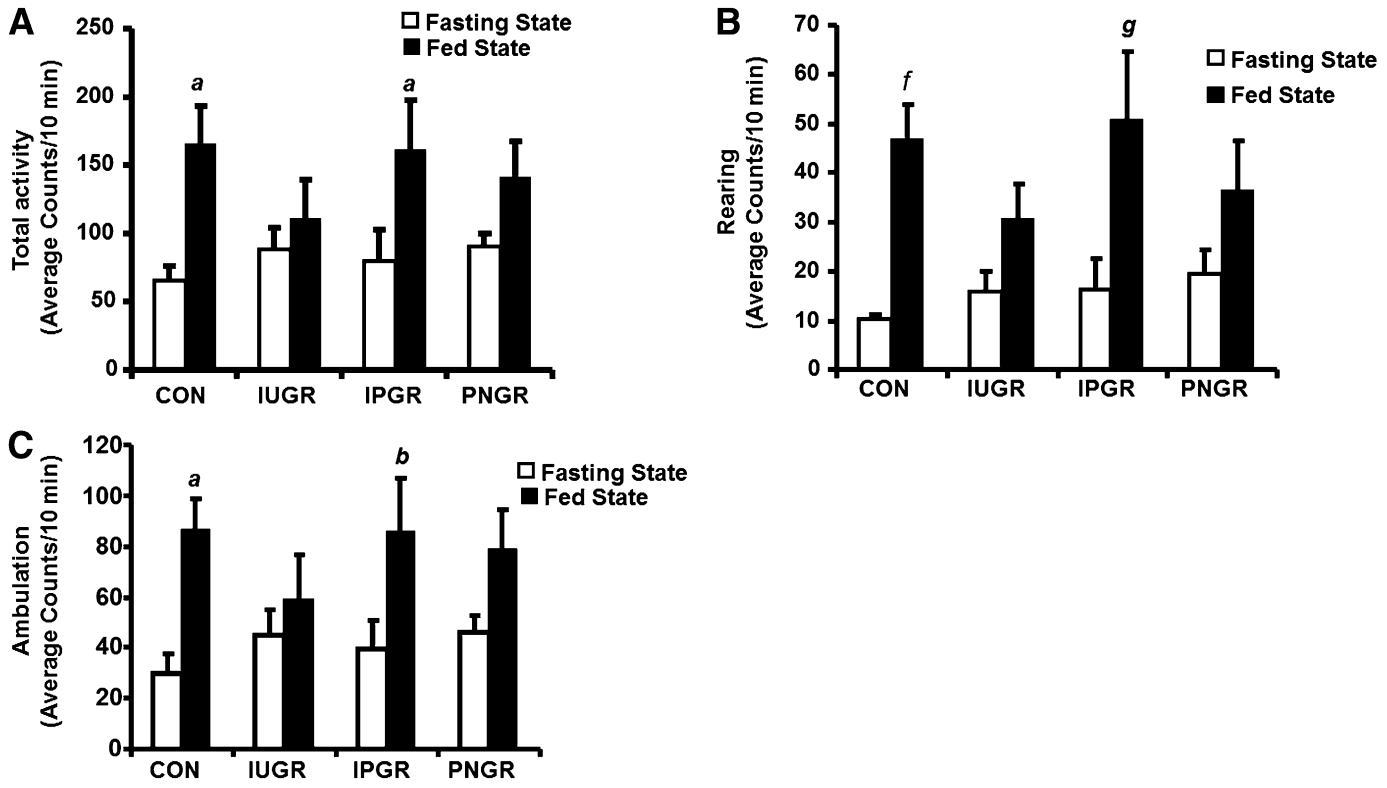

FIG. 4. Total activity (*A*), rearing activity (*B*), and total ambulatory activity (*C*) are shown in IUGR, IPGR, PNGR, and CON groups during fasting and fed states averaged as counts for 10-min epochs ($n = 6$ in each group). Fasting vs. fed states compared within the same group: $^{a}P < 0.01$, $^{b}P < 0.02$, $^{f}P < 0.001$, $^{g}P < 0.003$.

AUC of IPGR that was higher compared with that of PNGR ($P < 0.01$) but similar to that of CON (Fig. 5*D*).

Hyperinsulinemic-euglycemic clamp studies. Under basal conditions, the R_d and HGP were significantly higher in IPGR compared with CON ($P < 0.04$), IUGR ($P < 0.01$), and PNGR ($P < 0.01$) (Fig. 6*A* and *B*). During hyperinsulinemic-euglycemic clamp conditions, R_d in the IPGR group remained significantly greater than that in the CON ($P < 0.02$) and IUGR ($P < 0.01$) groups and increased from the corresponding basal R_d in the IPGR group ($P < 0.001$). The PNGR group exhibited increase in R_d during the hyperinsulinemic clamp compared with the corresponding basal R_d ($P < 0.001$) and that of the hyperinsulinemic-clamped IUGR group ($P < 0.01$). While HGP trended toward a decrease during the hyperinsulinemic clamp versus the corresponding basal value in all groups, a significant decrease was noted only in the IPGR group ($P < 0.05$) (Fig. 6*B*). The GIR and 2-deoxyglucose uptake in skeletal muscle (SKM) (soleus; oxidative type) were significantly increased in IPGR and PNGR compared with CON and IUGR ($P < 0.05$), supporting increased SKM insulin sensitivity and insulin-induced glucose uptake by oxidative muscle fibers (Fig. 6*C* and *D*). The GIR and 2-deoxyglucose uptake in SKM (soleus) of the IUGR was no different from that of CON. There were no intergroup differences observed in the insulin-induced glucose uptake by the extensor digitorum longus muscle (glycolytic type), gastrocnemius (mixed type), liver, or WAT (Fig. 6*D*).

DISCUSSION

This is a study examining the impact of metabolic programming in the adult male rat subjected to postnatal ad libitum feeding versus that of postnatal caloric restriction superimposed on intrauterine caloric restriction. IUGR led to an obese and metabolically inflexible but glucose tolerant and non–insulin resistant adult phenotype, while IPGR and PNGR displayed a lean, metabolically flexible, and highly insulin-sensitive phenotype (muscle and liver). IPGR demonstrated a higher glucose-induced insulin response compared with CON, resulting in normal glucose tolerance. This presentation in IPGR correlated with a higher resting oxygen consumption rate and physical activity level compared with CON, IUGR, and PNGR. Thus, it appears that postnatal nutrient restriction during lactation had a positive effect on the intrauterine calorie-restricted adult phenotype. This finding is novel in the backdrop of epidemiological observations of developing obesity and T2DM in low–birth weight infants with a flat postnatal growth pattern until 2 years of age followed by exponential growth between 2–8 years of age (15).

The increased visceral and subcutaneous fat and plasma leptin concentration in the IUGR group and absence of the same in IPGR and PNGR groups observed in our present study may underlie the observed metabolic profile. Normal insulin concentration and insulin-sensitive state of the 10-month-old male IUGR rat offspring may also promote triglyceride synthesis and storage in WAT. Previously, 9-month-old IUGR rat offspring subjected to ad libitum postnatal intake were observed to be heavier with increased adiposity by dual-energy X-ray absorptiometry and hypertriglyceridemia, with no change in lean body mass (7,16). Increased intra-abdominal adipose tissue is also reported from whole-body MRI obtained as early as term-corrected age in prematurely born low–birth weight human neonates with accelerated postnatal body weight gain (17,18).

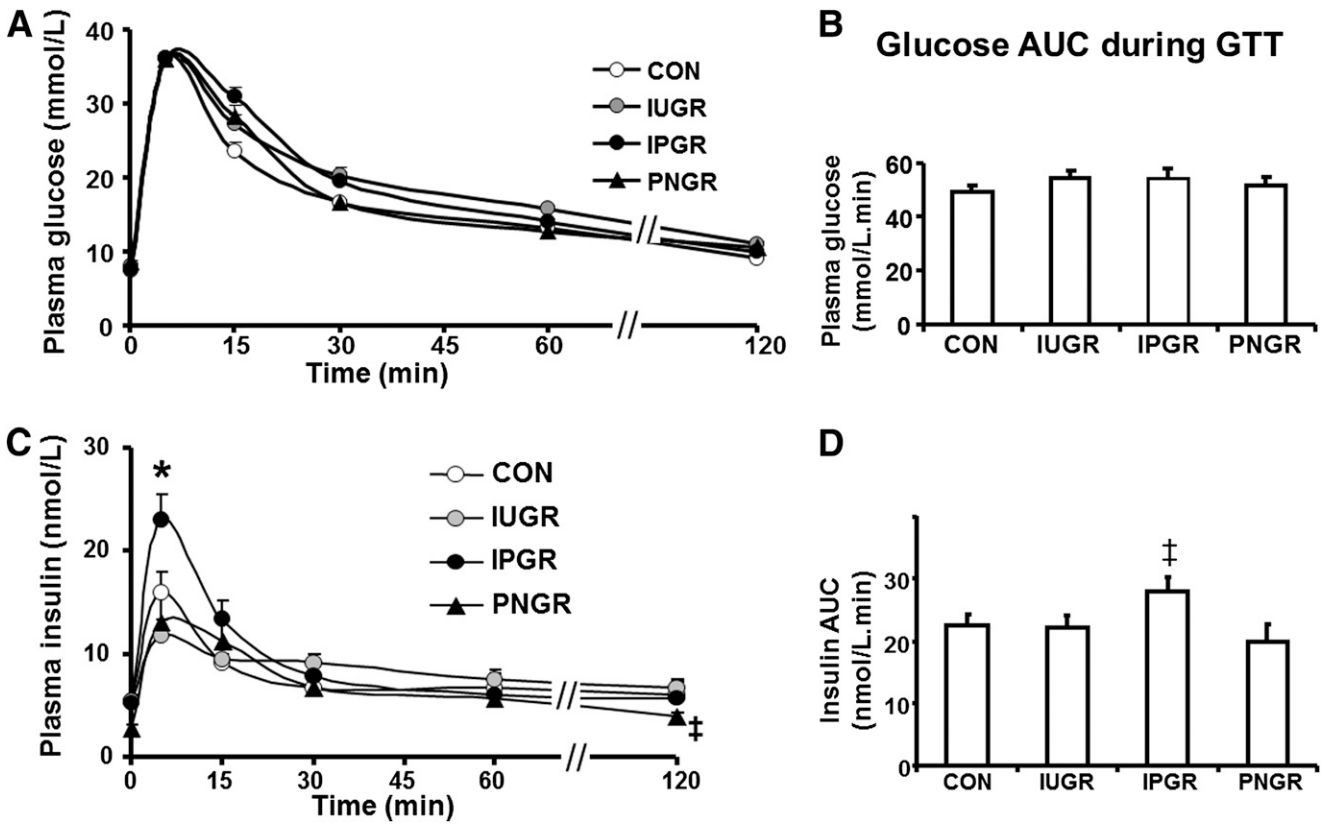

FIG. 5. *A*: Plasma glucose concentrations at baseline and 5, 15, 30, 45, 60, and 120 min after an intravenous glucose challenge are shown in CON, IUGR, PNGR, and IPGR (n = 7 each in all groups). *B*: AUC for plasma glucose concentration during the glucose tolerance test for CON, IUGR, PNGR, and IPGR. *C*: Plasma insulin concentrations at baseline and 5, 15, 30, 45, 60, and 120 min after an intravenous glucose challenge are shown in CON, IUGR, PNGR, and IPGR (n = 7 each in all groups). *P < 0.03 IPGR vs. CON, IUGR, and PNGR; ‡P < 0.05 IUGR vs. PNGR. *D*: The AUC for plasma insulin concentrations during the glucose tolerance test for CON, IUGR, PNGR, and IPGR; ‡P < 0.01 IPGR vs. PNGR.

The reason for visceral adiposity in insulin-sensitive IUGR remains unresolved in this study. Human adults demonstrating insulin sensitivity in the early stages of developing obesity have been described (19,20). One possible explanation is that even at 10 months of age, the insulin-sensitive state is responsible for promoting visceral adiposity. Once a certain threshold of adiposity is attained, insulin resistance may ensue. This explanation suggests that perhaps at a subsequent age (e.g., 15–17 months), insulin resistance may be evident that has not quite manifested at 10 months of age in the male IUGR offspring. An alternate explanation may be related to metabolic programming due to prenatal exposure to caloric restriction. Caloric restriction during a critical window of development may metabolically program the offspring permanently. Thus, a state of insulin deficiency due to caloric restriction during the fetal stage of development may have permanently programmed insulin sensitivity that persists during adult life despite acquisition of visceral adiposity. Such a state is uniquely different from that encountered in a normal adult animal exposed to a high-calorie diet, where adiposity and insulin resistance are seen (21). In the case of the latter explanation, insulin sensitivity is likely to persist at subsequent ages as well, warranting such investigations in the future to determine the reason behind the insulin-sensitive state in the adult IUGR male offspring.

Food intake per body weight in IUGR was lower than in CON, and V_{O_2} consumption failed to increase in the fed versus fasted states. In contrast, IPGR with no similar accumulation of visceral adipose tissue exhibited an improved metabolic profile with flexibility in postfeeding V_{O_2} and heat production. Therefore, while prenatal nutrient restriction resulted in heat production of both IUGR and IPGR similar to that of CON during fasting, only IUGR demonstrated decreased heat production (kilocalories per kilogram per hour) in the fed state compared with CON. PNGR with higher food intake per body weight and decreased caloric efficiency had an improved metabolic profile seen as an increase in V_{O_2} and heat production during the fed state mimicking IPGR and CON.

Activity level in the fed state of CON and IPGR increased significantly compared with the fasted state. In contrast, activity level in the fed state did not change significantly in the obese IUGR and lean PNGR groups compared with CON. The explanation for this observation may be related to either a central trigger in the hypothalamus (22) or peripheral skeletal muscle fiber type changes, each being specific to IUGR versus PNGR groups. The ultimate phenotype of obesity is due to a diminution of energy expenditure and physical activity despite reduced caloric intake in the adult male IUGR offspring. While exercise may augment energy expenditure and further enhance insulin sensitivity in the IUGR depending on the intensity of training and amount of exercise (23,24), it is not clear whether this intervention would further benefit the PNGR that already exhibits augmented energy expenditure and enhanced insulin sensitivity with increased insulin-stimulated glucose uptake in the soleus. Additional differences observed in the resting V_{O_2} revealed IUGR to display the least oxygen consumption independent of physical activity

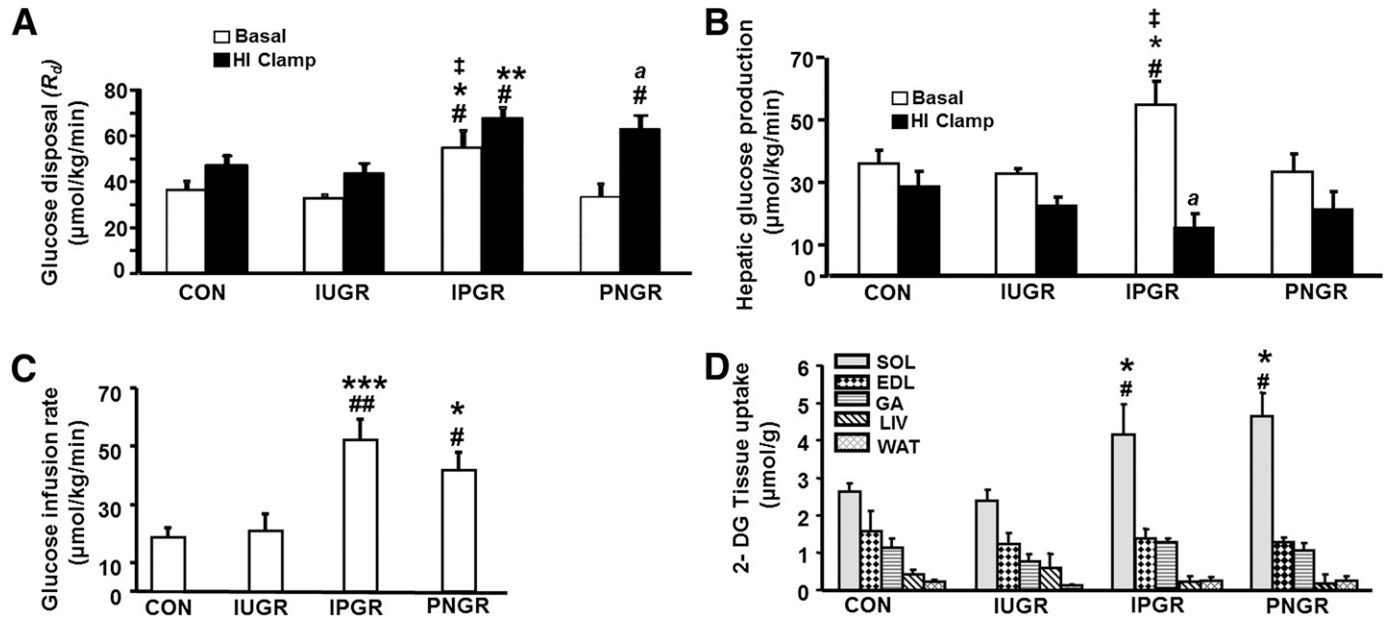

FIG. 6. *A*: Whole-body insulin sensitivity with R_d under basal conditions and during hyperinsulinemic-euglycemic (HI) clamp in all groups (n = 6 each in all groups). *P < 0.04 vs. CON; **P < 0.02 vs. CON; #P < 0.01 vs. IUGR; ‡P < 0.01 vs. PNGR; [a]P < 0.001 R_d under basal vs. hyperinsulinemic-euglycemic clamp conditions. *B*: HGP under basal and during hyperinsulinemic-euglycemic clamp conditions in all groups (n = 6 each in all groups). *P < 0.04 vs. CON; #P < 0.01 vs. IUGR; ‡P < 0.01 vs. PNGR; [a]P < 0.001 HGP under basal vs. hyperinsulinemic-euglycemic clamp conditions. *C*: Insulin sensitivity with GIR during the hyperinsulinemic-euglycemic clamp condition in all groups (n = 6 each). *P < 0.04 vs. CON; ***P < 0.003 vs. CON; #P < 0.04 vs. IUGR; ##P < 0.003 vs. IUGR. *D*: Insulin-stimulated glucose uptake in skeletal muscles, liver (LIV), and WAT in all groups is shown (n = 6 each in all groups). DG, deoxyglucose; EDL, extensor digitorum longus muscle; GA, gastrocnemius; SOL, soleus. *P < 0.04 vs. CON; #P < 0.04 vs. IUGR.

compared with the lean IPGR and PNGR groups. Thus, exercise may only show partial benefit in the IUGR group as well. Collectively, these findings related to the metabolic and energy profiles and activity level situate the PNGR group in between the IUGR (low) and IPGR (high) groups.

The whole-body glucose metabolism examined by hyperinsulinemic-euglycemic clamp studies did not show any significant differences in R_a, HGP, or GIR between IUGR and CON confirming an insulin-sensitive state in the former. Additionally, there was no hyperglycemia or hyperinsulinemia by intravenous glucose tolerance test. These findings in freely moving rats are similar to those of previous reports in anesthetized 260-day-old male IUGR rats that were shown to maintain insulin sensitivity by in vivo hyperinsulinemic-euglycemic clamp studies (6). The IPGR group demonstrated enhanced whole-body insulin sensitivity with higher R_a and GIR during basal and hyperinsulinemic clamp conditions compared with all the other groups. The PNGR group displayed such an increase in R_d only under hyperinsulinemic-euglycemic clamp conditions. Higher HGP in IPGR under basal condition that was suppressed during hyperinsulinemic clamp may reflect the liver's response (R_a) at attempting to match the higher whole-body demand for glucose (R_d) in the more active IPGR group, also reflected as enhanced hepatic insulin sensitivity and skeletal muscle glucose uptake. In contrast, the PNGR group did not demonstrate such changes in HGP, while expressing increased insulin sensitivity in other tissues (GIR changes reflecting those of skeletal muscle–soleus glucose uptake).

While other groups using the gestational caloric restriction rat model have previously reported in vivo insulin resistance in the adult IUGR male offspring, these conclusions were based on ratios between circulating glucose and insulin concentrations alone (25). Similarly, in a comparison of two other rat IUGR models present in the literature with our model described here, it appears that the utero-placental insufficiency rat model of IUGR results in hepatic insulin resistance with no change in glucose utilization at an early age of 3–6 months (5) and increased visceral adipose tissue in 21-day-old males (26). The protein-restricted IUGR male offspring demonstrates in vitro changes that are consistent with insulin resistance in skeletal muscle and WAT (27); however, no in vivo hyperinsulinemic-euglycemic clamp studies exist to date. A decrease in pancreatic β-cell mass and their replication was previously shown in the IUGR offspring at 21 days of age (28). In a compilation of these studies together, it appears that none of these studies demonstrated changes in in vivo glucose utilization consistent with insulin resistance; rather, some investigations demonstrated early insulin deficiency or relied on ratios between glucose and insulin to make conclusions regarding the presence of insulin resistance subsequently in the adult offspring. Using hyperinsulinemic-euglycemic clamp experiments conducted systematically along with assessment of tissue glucose uptake in the current study, we have observed insulin sensitivity despite visceral adiposity in the adult IUGR male offspring.

In conclusion, the male IUGR adult rat offspring at the age of 10 months demonstrates visceral and subcutaneous adiposity, metabolic inflexibility between fasting and fed states, and decreased activity while remaining insulin sensitive in the fed state. In contrast, the adult male IPGR offspring remain lean, demonstrate enhanced insulin sensitivity, metabolic flexibility, and increased resting V_{O_2} and activity in the fed state. PNGR offspring remain lean and insulin sensitive and demonstrate caloric inefficiency despite metabolic flexibility but without an increase in activity during the fed state. Therefore, postnatal caloric restriction superimposed on IUGR improved the metabolic profile, while unrestricted access to calories in the IUGR offspring

promoted metabolic inflexibility and visceral adiposity prior to the development of insulin resistance or overt diabetes. Similar systematic studies at a subsequent age in the adult IUGR male offspring are warranted to determine whether the state of insulin resistance with or without glucose intolerance sets in much later in life. We speculate that our study provides the basis for exploring postnatal nutritional interventions targeting "catch-up growth" in future clinical trials.

ACKNOWLEDGMENTS

This work was supported by grants from the *Eunice Kennedy Shriver* National Institute of Child Health and Human Development (41230 and 25024).

No potential conflicts of interest relevant to this article were reported.

M.G. performed and assisted in metabolic chamber studies, glucose tolerance tests, hyperinsulinemic-euglycemic clamp experiments, and assays of glucose, insulin, and leptin; undertook data analysis; and wrote the manuscript. M.T. performed studies in the metabolic chamber and abdominal computed tomography and assisted with glucose tolerance tests and clamp studies. Y.D. performed hyperinsulinemic-euglycemic clamp experiments and undertook data analysis for clamps and tissue glucose uptake experiments. S.T. and B.-C.S. provided assistance with creating the animal model, weight monitoring, dietary interventions, food and water intake, and the hyperinsulinemic-euglycemic clamp experiments. D.S. assisted with performing the abdominal computed tomography at the Crump Institute for Molecular Imaging. S.U.D. developed the animal model, developed and provided guidance and oversight for the entire study design and methods, critically reviewed the analyses and results, contributed to the introduction and the presentation of observations and discussion, edited multiple drafts of the manuscript, and undertook the entire revision of the manuscript in response to the reviewers and editors. S.U.D. is the guarantor of this work and, as such, had full access to all the data in the study and takes responsibility for the integrity of the data and the accuracy of the data analysis.

REFERENCES

1. Ozanne SE, Jensen CB, Tingey KJ, Storgaard H, Madsbad S, Vaag AA. Low birthweight is associated with specific changes in muscle insulin-signalling protein expression. Diabetologia 2005;48:547–552
2. Oak SA, Tran C, Pan G, Thamotharan M, Devaskar SU. Perturbed skeletal muscle insulin signaling in the adult female intrauterine growth-restricted rat. Am J Physiol Endocrinol Metab 2006;290:E1321–E1330
3. Thamotharan M, Shin BC, Suddirikku DT, Thamotharan S, Garg M, Devaskar SU. GLUT4 expression and subcellular localization in the intrauterine growth-restricted adult rat female offspring. Am J Physiol Endocrinol Metab 2005;288:E935–E947
4. Garg M, Thamotharan M, Rogers L, Bassilian S, Lee WN, Devaskar SU. Glucose metabolic adaptations in the intrauterine growth-restricted adult female rat offspring. Am J Physiol Endocrinol Metab 2006;290:E1218–E1226
5. Vuguin P, Raab E, Liu B, Barzilai N, Simmons R. Hepatic insulin resistance precedes the development of diabetes in a model of intrauterine growth retardation. Diabetes 2004;53:2617–2622
6. Thompson NM, Norman AM, Donkin SS, et al. Prenatal and postnatal pathways to obesity: different underlying mechanisms, different metabolic outcomes. Endocrinology 2007;148:2345–2354
7. Desai M, Babu J, Ross MG. Programmed metabolic syndrome: prenatal undernutrition and postweaning overnutrition. Am J Physiol Regul Integr Comp Physiol 2007;293:R2306–R2314
8. Krechowec SO, Vickers M, Gertler A, Breier BH. Prenatal influences on leptin sensitivity and susceptibility to diet-induced obesity. J Endocrinol 2006;189:355–363
9. Eriksson J, Forsén T, Tuomilehto J, Osmond C, Barker D. Size at birth, fat-free mass and resting metabolic rate in adult life. Horm Metab Res 2002;34:72–76
10. Yoshizumi T, Nakamura T, Yamane M, et al. Abdominal fat: standardized technique for measurement at CT. Radiology 1999;211:283–286
11. Westbrook R, Bonkowski MS, Strader AD, Bartke A. Alterations in oxygen consumption, respiratory quotient, and heat production in long-lived GHRKO and Ames dwarf mice, and short-lived bGH transgenic mice. J Gerontol A Biol Sci Med Sci 2009;64:443–451
12. Bates SH, Dundon TA, Seifert M, Carlson M, Maratos-Flier E, Myers MG Jr. LRb-STAT3 signaling is required for the neuroendocrine regulation of energy expenditure by leptin. Diabetes 2004;53:3067–3073
13. Livesey G, Elia M. Estimation of energy expenditure, net carbohydrate utilization, and net fat oxidation and synthesis by indirect calorimetry: evaluation of errors with special reference to the detailed composition of fuels. Am J Clin Nutr 1988;47:608–628
14. Lusk G. Analysis of the oxidation of mixtures of carbohydrate and fat. J Biol Chem 1924;54:41–42
15. Eriksson JG, Osmond C, Kajantie E, Forsén TJ, Barker DJ. Patterns of growth among children who later develop type 2 diabetes or its risk factors. Diabetologia 2006;49:2853–2858
16. Desai M, Gayle D, Babu J, Ross MG. The timing of nutrient restriction during rat pregnancy/lactation alters metabolic syndrome phenotype. Am J Obstet Gynecol 2007;196:555.e1–e7
17. Cooke RJ, Griffin I. Altered body composition in preterm infants at hospital discharge. Acta Paediatr 2009;98:1269–1273
18. Uthaya S, Thomas EL, Hamilton G, Doré CJ, Bell J, Modi N. Altered adiposity after extremely preterm birth. Pediatr Res 2005;57:211–215
19. Kahn BB, Flier JS. Obesity and insulin resistance. J Clin Invest 2000;106:473–481
20. Patti ME, Kahn BB. Nutrient sensor links obesity with diabetes risk. Nat Med 2004;10:1049–1050
21. Akiyama T, Tachibana I, Shirohara H, Watanabe N, Otsuki M. High-fat hypercaloric diet induces obesity, glucose intolerance and hyperlipidemia in normal adult male Wistar rat. Diabetes Res Clin Pract 1996;31:27–35
22. Shin B, Dai Y, Thamotharan M, Gibson LC, Devaskar SU. Pre and post natal calorie restriction perturbs early hypothalamic neuropeptide and energy balance. J Neurosci Res. 2 March 2012 [Epub ahead of print]
23. Haram PM, Kemi OJ, Lee SJ, et al. Aerobic interval training vs. continuous moderate exercise in the metabolic syndrome of rats artificially selected for low aerobic capacity. Cardiovasc Res 2009;81:723–732
24. Garg M, Thamotharan M, Oak SA, et al. Early exercise regimen improves insulin sensitivity in the intrauterine growth-restricted adult female rat offspring. Am J Physiol Endocrinol Metab 2009;296:E272–E281
25. Vickers MH, Reddy S, Ikenasio BA, Breier BH. Dysregulation of the adipoinsular axis—a mechanism for the pathogenesis of hyperleptinemia and adipogenic diabetes induced by fetal programming. J Endocrinol 2001;170:323–332
26. Joss-Moore LA, Wang Y, Campbell MS, et al. Uteroplacental insufficiency increases visceral adiposity and visceral adipose PPARgamma2 expression in male rat offspring prior to the onset of obesity. Early Hum Dev 2010;86:179–185
27. Zambrano E, Bautista CJ, Deás M, et al. A low maternal protein diet during pregnancy and lactation has sex- and window of exposure-specific effects on offspring growth and food intake, glucose metabolism and serum leptin in the rat. J Physiol 2006;571:221–230
28. Matveyenko AV, Singh I, Shin BC, Georgia S, Devaskar SU. Differential effects of prenatal and postnatal nutritional environment on ß-cell mass development and turnover in male and female rats. Endocrinology 2010;151:5647–5656